Transport of Probe Particles in Semidilute Polymer Solutions

X. Ye[†] and P. Tong*

Department of Physics, Oklahoma State University, Stillwater, Oklahoma 74078

L. J. Fetters

Exxon Research and Engineering Company, Route 22 East, Annandale, New Jersey 08801

Received February 5, 1998; Revised Manuscript Received June 23, 1998

ABSTRACT: Dynamic light scattering and sedimentation measurements are carried out to study the motion of probe particles in neutral and adsorbing polymer solutions. By varying the microscopic interaction between the colloidal particle and the polymer molecule, we observe three different behaviors to the Stokes−Einstein (SE) equation in the same colloid−polymer system. The measurements clearly delineate the sample conditions under which the three different behaviors are observed, respectively. It is shown that the three different behaviors can be explained consistently in terms of the microstructures formed in the colloid−polymer mixture. The experiment demonstrates the importance of restraining the particle−medium interaction in the measurement of the microrheological properties of complex fluids.

I. Introduction

In recent years there has been a growing interest in studying microrheological properties of complex fluids containing macromolecules of different architectures. Examples include gels,[1,2] foams,[3] emulsions,[4] and various biomaterials, such as DNA, polymeric actin, and cell extracts.[5,6] The study of local viscoelastic properties of these biomaterials at scales comparable to the molecular dimensions is of fundamental interest in statistical physics and is also relevant to many biological processes, such as cell morphogenesis, locomotion, division, and macromolecular transport.[7,8] Various experimental techniques have been developed recently for the study of the microrheological properties, and many of them involve the measurement of the motion of probe particles suspended in the medium of interest.[1,9−12] In this paper, we focus on the transport of probe particles in semidilute polymer solutions. The colloid−polymer system is simpler, because the particles behave like hard spheres and the polymer chains form a fluctuating network, whose spatial structure has been intensively studied for many years and now is well understood.[13] Many theoretical and experimental investigations have been carried out to study the motion of small particles in various aqueous and organic polymer solutions.[14−22] While some progress has been made in understanding the colloidal transport in polymer solutions, the experimental situation, however, is complicated by the polymer adsorption, electrostatic interactions, and other effects that are peculiar to the system under study.[17]

The main issue in the colloidal transport is to understand how particle−particle and particle−polymer interactions affect the frictional force experienced by the particles.[15,23] For a dilute colloidal suspension, the interaction between the particles can be ignored and the particle−polymer interaction becomes a dominant factor to determine the transport of the particles in polymer solutions. The frictional force experienced by the particles can be expressed by the microscopic viscosity η_c of the polymer solution. (Hereafter, we will use the subscripts c and p to refer to the colloid and polymer, respectively.) The local viscosity η_c differs from the macroscopic viscosity η_p of the polymer solution, which is usually measured by a large-size viscometer. The solution viscosity η_p represents an effective viscosity when the medium is treated as a viscous continuum. Therefore, η_p is a scale invariant quantity, so long as the length scale involved is larger than the correlation length ξ of the polymer solution, which describes the average mesh size of the fluctuating polymer network. When the relevant length scale becomes comparable to or smaller than ξ, the polymer solution cannot be treated as a continuum anymore and its local viscosity η_c may change with the length scale at which it is probed.[13,16]

In the experiment, η_c can be obtained by measuring either the diffusion constant D_c or the sedimentation velocity v_c of the particles suspended in the polymer solution. Laser light scattering and centrifugation techniques have been used to measure D_c and v_c, respectively. The measured D_c is related to η_c via the Stokes−Einstein relation[24]

$$D_c(C_p) = \frac{k_B T}{6\pi\eta_c(C_p)R_h} \tag{1}$$

where k_BT is the thermal energy and R_h is the hydrodynamic radius of the particle. In the dilute suspension, the Stokes velocity v_c is given by[23]

$$v_c(C_p) = \frac{2R_h^2\Delta d A}{9\eta_c(C_p)} \tag{2}$$

where A is the centripetal acceleration and Δd is the density difference between the particle and the solvent. Because adding polymer into the suspension increases the overall viscosity of the solution, the microscopic viscosity $\eta_c(C_p)$ [and hence $D_c(C_p)$ and $v_c(C_p)$] may also change with the polymer concentration C_p.

* To whom correspondence should be addressed. E-mail: ptong@osuunx.ucc.okstate.edu.

[†] Also at Department of Physics, Northeastern University, Shenyang, People's Republic of China.

S0024-9297(98)00172-7 CCC: $15.00
Published on Web 08/08/1998

Equations 1 and 2 are obtained originally for noninteracting spheres suspended in a solvent of small molecules. For colloidal particles suspended in a polymer solution, these equations can be used to define $\eta_c(C_p)$ even when the size of the particles becomes comparable to or smaller than the characteristic length scale of the polymer solution. Care must be taken, however, that the relationship between D_c (or v_c) and η_c is unique only when the other parameters in the equation, such as R_h, remain unchanged under different solution conditions. For example, if the polymer molecules interact attractively with the particles, the adsorption of the polymer chains onto the colloidal surface may change the value of R_h. If the polymer adsorption produces a polymer−colloid network in the solution, the hydrodynamic radius R_h is not even well-defined. Under these circumstances, eqs 1 and 2 may not be applicable. Previous light scattering experiments have found deviations from the Stokes−Einstein (SE) relation in various colloid−polymer mixtures.[14−22] These deviations can be divided into three groups: positive deviations from the SE behavior when $D_c(C_p)\eta_p/(D_c(0)\eta_0) > 1$, negative deviations from the SE behavior when $D_c(C_p)\eta_p/(D_c(0)\eta_0) < 1$, and adherence to the SE equation when $D_c(C_p)\eta_p/(D_c(0)\eta_0) = 1$. Here $D_c(0)$ is the particle diffusion constant in the pure solvent and η_0 is the solvent viscosity. A brief review of the literature has been given by Won et al.[14]

While different mechanisms have been proposed to explain the deviations from the SE relation,[20] they are not consistent with each other and they usually can only explain one of the behaviors but not the others. A coherent picture is certainly needed in order to provide a consistent theory to explain the phenomena as a whole. The lack of a coherent theory is partially due to the fact that the colloid−polymer interaction in the systems under study is not exactly known. In this paper, we present light scattering and sedimentation measurements in a well-characterized colloid−polymer system, in which the particles are approximately hard spheres and the microscopic interaction between the particle and the polymer molecule can be tuned to be either repulsive or attractive. By varying the colloid−polymer interaction, we observe the three different behaviors toward the SE equation in the same colloid−polymer system. Because the basic molecular interactions are chosen to be simple, we are able to delineate the sample conditions under which the three different behaviors are observed, respectively. The experiment demonstrates that the three different behaviors to the SE equation can all be explained consistently in terms of the microstructures formed in the colloid−polymer mixture.

The remainder of the paper is organized as follows. Experimental details are described first in section II, and then the light scattering and sedimentation results are discussed in section III. Finally, the work is summarized in section IV.

II. Experimental Methods

The colloid−polymer system chosen for the study has been well characterized previously using various scattering techniques and has been detailed elsewhere.[25−29] Here we only mention some key points. The colloidal particle consists of a calcium carbonate ($CaCO_3$) core with an adsorbed monolayer of a randomly branched calcium alkylbenzenesulfonate surfactant. The average density of the particle is $d_c \simeq 2.0$ g/cm^3. The colloidal samples are prepared by diluting known amounts of the concentrated suspension with the solvent, decane. The resulting suspension is found to be relatively monodispersed with an average $R_h = 5$ nm and ~10% standard deviation.[25] Our recent small angle neutron scattering measurements[27] have revealed that the particle has a core radius of $R_0 = 2.0$ nm and a surfactant monolayer thickness of $\delta = 2.0$ nm. Thus the static (or mass) radius of the particle is $R_m = R_0 + \delta = 4.0$ nm. Measurements of the particle structure factor have shown that the colloidal suspension behaves like a hard-sphere system.[26,27]

The polymers used in the experiment are hydrogenated polyisoprene (poly(ethylenepropylene) or PEP) and its end-functionalized derivative amine-PEP, which contains a tertiary amino group capped at one end of the chain. The parent PEP and its end-functionalized derivative are model polymers ($M_w/M_n < 1.1$), which have been well characterized previously using various experimental techniques.[30−32] Decane is used as the solvent because it is a good solvent for both the colloid and the polymers. The density of decane is $d_s = 0.73$ g/cm^3 and its viscosity $\eta_0 = 0.838$ cP at 25 °C. Recent scattering experiments[28,34] have shown that the pure amine-PEP−decane solution behaves the same as the PEP−decane solution with no association found in the amine-PEP−decane solution. Using a capillary viscometer, Davidson et al.[32] have measured the viscosity of the polymer solution as a function of C_p (g/cm^3). They found that the ratio of the solution viscosity η_p to the solvent viscosity η_0 can be well described by

$$\eta_p/\eta_0 = 1 + [\eta]C_p + k_H([\eta]C_p)^2 \qquad (3)$$

where the polymer intrinsic viscosity $[\eta] = 2.05 \times 10^{-2} M_p^{0.73}$ cm^3/g and the Huggins coefficient $k_H = 0.35$. In the viscosity measurements, the polymer concentration was varied up to the overlap concentration C^*.[32−34]

Sedimentation measurements are conducted using a commercial ultracentrifuge (Beckman Model L8-70M). Experimental details have been given elsewhere[35,36] and here we only mention a few key points. The mixture samples are centrifuged at a rotation rate $f = 35\,000$ rpm for 4−12 h depending on the sample viscosity. The corresponding centripetal acceleration $A \simeq 1.5 \times 10^8$ cm/s^2 (1.5×10^5 g), which is large enough to cause the particles to settle 1−5 cm toward the bottom of the cell. After the centrifugation, a sharp interface can be observed by eye in the initially uniform solution. This interface separates the upper clear solvent region from the lower dark-brown colloid-rich region. The traveling distance h of the interface is measured by a low-magnification microscope, which is mounted on a vertical translation stage controlled by a micrometer. The experimental uncertainties for the measured h are less than 5%. The particle settling velocity is obtained via $v_c = h/t$, where t is the centrifugation time. All the sedimentation measurements are conducted at 22 °C. The colloid volume fraction of the samples is fixed at $\phi_c = 0.014$. This is the lowest colloid concentration at which one can still observe the sedimentation interface visually. We have verified that at this volume fraction the interaction between the particles can be ignored.[35,36] Because the polymer density ($d_p = 0.856$ g/cm^3) is fairly close to that of decane, polymer sedimentation during the centrifugation is negligible.[36]

Light scattering measurements are performed using a scattering goniometer (Brookhaven Instruments BI-200SM) at room temperature. A 30-mW He/Ne laser (Spectra Physics, Model 127) illuminates a 10-mL sample tube in an index-matching vat. Decalin is used as an index-matching fluid to reduce stray scattering from the cylindrical glass wall. The scattered light coming from a well-defined scattering volume and angular aperture is collected by a photomultiplier (EMI 9863). A multi-τ digital correlator (ALV-5000) is used to measure the intensity autocorrelation function $g(t)$. We have verified that the decay rate Γ_c of the measured $g(t)$ for the pure colloid and mixture samples shows the expected Q^2 dependence on the scattering wavenumber $Q = (4\pi n/\lambda_0)\sin(\theta/2)$. Here θ is the scattering angle, n is the refractive index of the solvent, and λ_0 is the wavelength of the incident light. To save space,

we present only the correlation measurements at $\theta = 90°$ in section III.

To measure the correlation length ξ of the polymer solution, we conduct small-angle neutron scattering (SANS) measurements for the pure PEP samples in deuterated decane. The measurements are made on a SANS instrument (NG-7) at the National Institute of Standards and Technology. The incident neutron wavelength $\lambda_0 = 5.00 \pm 0.35$ Å, and the usable Q range is $0.01\ \text{Å}^{-1} \leq Q \leq 0.142\ \text{Å}^{-1}$. The scattered neutron intensity is collected by a two-dimensional detector. All the neutron scattering measurements are made at room temperature. Standard procedures are followed to obtain the normalized intensity $I(Q)$ relative to an isotropic scattering standard.[26,27]

III. Results and Discussion

A. Probe Particles in a Nonadsorbing Polymer Solution. We first discuss the sedimentation measurements of the colloidal particles suspended in the PEP solution. Our previous light and neutron scattering measurements on the fresh mixture samples (less than 2 months old) have shown[25,29] that the PEP chains do not adsorb onto the colloidal surfaces. As will be discussed in section IIIC, the PEP chains start to adsorb onto the colloidal particles in the old mixture samples (more than 6 months old) and form cross-linked polymer−colloid clusters in the solution. However, the kinetics of the adsorption and aggregation is so slow that the fresh samples can be treated as being at quasi-equilibrium. In the mixture of a colloid and a nonadsorbing polymer, the free polymer molecules can introduce a depletion attraction between the particles.[37] This polymer-induced attraction was indeed found in the colloid−PEP mixture when the colloid concentration is high.[26,27] For the dilute colloidal suspension with $\phi_c = 0.014$, the depletion interaction is found to be negligible.[36] The colloid−PEP mixture samples used in the sedimentation measurements are all fresh ones prepared within 1−2 weeks. Because there is no adsorption in these fresh samples, the particle's R_h remains unchanged in the PEP solution. Therefore, η_c in eq 2 is uniquely defined. To reduce systematic errors in the experiment, we present the sedimentation data in terms of the velocity ratio $v_c(C_p)/v_c(0)$ [or $v_c(0)/v_c(C_p)$].

Figure 1a shows the measured $v_c(C_p)\eta_p/[v_c(0)\eta_0]$ as a function of C_p for the PEP with $M_p = 17\,500$ (circles) and $M_p = 26\,000$ (squares) [in atomic mass units, same afterward]. From eq 2 one finds that $v_c(C_p)\eta_p/[v_c(0)\eta_0]$ equals the viscosity ratio $\eta_p(C_p)/\eta_c(C_p)$, where $\eta_p(C_p)$ is the solution viscosity given in eq 3. The effect of adding polymer is pronounced. The measured $\eta_p(C_p)/\eta_c(C_p)$ shows large positive deviations from unity (the dashed line). At low polymer concentrations, the measured $\eta_p(C_p)/\eta_c(C_p)$ increases with C_p up to a maximum value when C_p reaches a crossover value $\tilde{C}_p \simeq 0.07$ g/cm^3. Above $\tilde{C}_p$, the measured $\eta_p(C_p)/\eta_c(C_p)$ starts to decay back to unity. To find the cause for the positive deviations from the SE behavior, we analyze the sedimentation data in another way. Figure 1b shows the measured $v_c(0)/v_c(C_p)$ as a function of C_p for the PEP with $M_p = 26\,000$. From eq 2 we have $v_c(0)/v_c(C_p) = \eta_c/\eta_0$. It is seen that the measured η_c/η_0 first increases linearly with C_p up to $\tilde{C}_p$ and then turns up sharply. The solid curve is the solution viscosity $\eta_p(C_p)$ measured by Davidson et al. (see eq 3). The dashed line is the linear part of the measured viscosity $\eta_p/\eta_0 = 1 + [\eta]C_p$. Figure 1b thus reveals that the probe particles in the polymer solution "feel" the linear viscosity when $C_p < \tilde{C}_p$, and they experience the solution viscosity when $C_p \gg \tilde{C}_p$. Similar behavior of η_c/η_0 was also observed for the PEP with other molecular weights ranging from 17 500 to 88 000.[35] It was found that the crossover concentration $\tilde{C}_p$ remains constant independent of M_p.

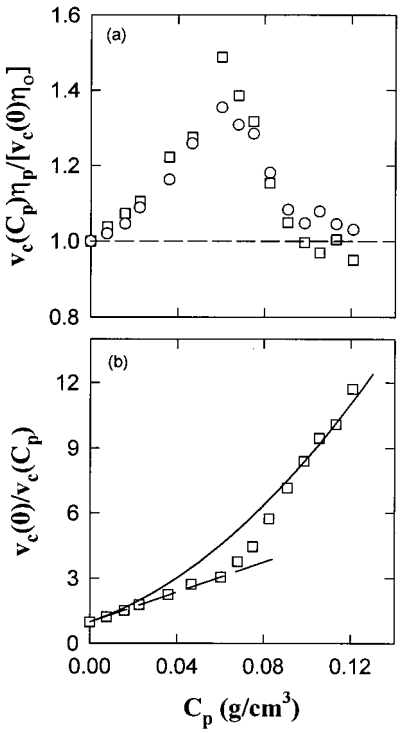

Figure 1. (a) Measured $v_c(C_p)\eta_p/[v_c(0)\eta_0]$ as a function of C_p for the colloid−PEP mixture samples with $M_p = 17{,}500$ (circles) and $M_p = 26{,}000$ (squares). The dashed line indicates a constant baseline of unity. (b) Measured $v_c(0)/v_c(C_p)$ as a function of C_p for the colloid−PEP mixture samples with $M_p = 26{,}000$. The solid curve shows the viscosity of the polymer solution and the dashed line is the linear viscosity $\eta_p/\eta_0 = 1 + [\eta]C_p$.

To understand the physical meaning of $\tilde{C}_p$, we calculate the polymer correlation length $\xi \simeq R_g(C_p/C^*)^{-3/4}$ at this concentration.[13] Here $C^* = M_p/[(4\pi/3)R_g^3]$ is the polymer overlap concentration and R_g is the radius of gyration of the polymer chains. Because $R_g \sim M_p^{3/5}$, ξ is a decreasing function of C_p and is independent of M_p. Increasing C_p in the experiment, therefore, becomes equivalent to reducing the value of ξ. For the PEP with $M_p = 26{,}000$, its $R_g = 8.3$ nm.[27] Thus we have $C^* = 0.018$ g/cm^3 and $\xi \simeq 3$ nm when $C_p = \tilde{C}_p$. If $1/[\eta]$ is used to define C^*, we find $C^* = 0.0292$ g/cm^3 and the corresponding $\xi \simeq 4.3$ nm at $\tilde{C}_p$. This value of ξ is very close to the particle's hydrodynamic radius R_h (5.0 nm). As mentioned in the above, R_h is ∼20% larger than the mass radius R_m (4 nm).

To further verify the above calculation, we directly measure ξ for the pure PEP in deuterated decane. In the SANS experiment, the scattered neutron intensity $I(Q)$ is measured as a function of Q. It has been shown that $I(Q)$ has the Lorentzian form[38,39]

$$\frac{C_p}{I(Q)} \propto 1 + \frac{1}{3}(Q\xi)^2 + \ldots \qquad (4)$$

where the numerical factor $^1/_3$ is introduced such that ξ becomes equal to R_g in the dilute limit. Figure 2a shows the measured $C_p/I(Q)$ as a function of Q^2 for the pure PEP solution at $C_p = 0.0038$ g/cm^3 (circles) and 0.063 g/cm^3 (squares). It is seen that in the small-Q

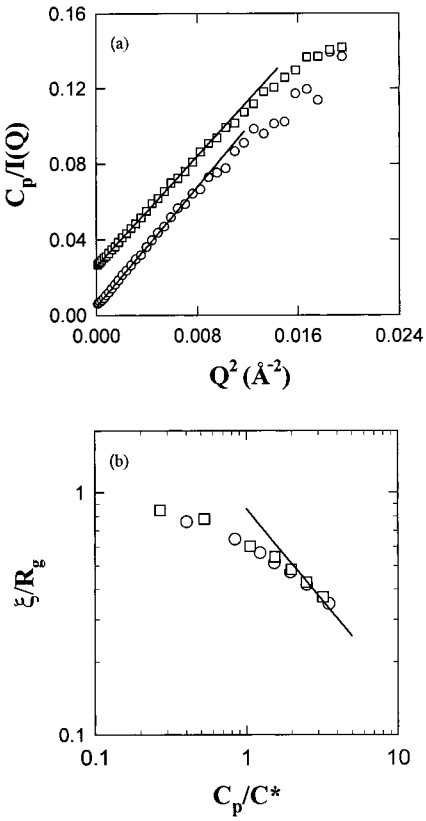

Figure 2. (a) Measured $C_p/I(Q)$ as a function of Q^2 for the pure PEP ($M_p = 26{,}000$) in deuterated decane with $C_p = 0.0038$ g/cm^3 (circles) and $C_p = 0.063$ g/cm^3 (squares). The solid lines are the linear fits to the data. (b) Normalized correlation length ξ/R_g as a function of C_p/C^* for the pure PEP samples with $M_p = 26{,}000$ (circles) and $M_p = 33{,}000$ (squares). The solid line shows the extrapolated power law $\xi/R_g = 0.86(C_p/C^*)^{-3/4}$.

region the scattering data can be well described by a linear function (the solid lines), from which one obtains ξ using eq 4. Note that the linear region for the high-C_p sample is wider, indicating that ξ is decreased at the higher polymer concentration. Figure 2b shows the normalized correlation length ξ/R_g as a function of C_p/C^* for the PEP samples with $M_p = 26{,}000$ (circles) and $M_p = 33{,}000$ (squares). Here we have used $C^* = M_p/[(4\pi/3)R_g{}^3]$ as the definition of the overlap concentration (same afterward). It has been shown that the ratio ξ/R_g is a universal function of C_p/C^* independent of M_p.[38,39] The solid line in Figure 2b shows the extrapolated power law $\xi/R_g = 0.86(C_p/C^*)^{-3/4}$, which has been well tested in other polymer solutions.[38,39] The SANS measurements, therefore, further support the above numerical calculation of ξ.

Many years ago de Gennes and his co-workers[13,16] proposed that when R_h is smaller than ξ, the particles move easily in the polymer solution and they "feel" only the solvent viscosity η_0, i.e., $\eta_c/\eta_0 = 1$. When $R_h \gg \xi$, the particles are trapped and η_c/η_0 becomes equal to η_p/η_0. In the transition region, η_c/η_0 is expected to be a scaling function $\varphi(R_h/\xi)$, which depends only on C_p and is independent of M_p. In a recent sedimentation experiment,[35] we measured η_c/η_0 at various polymer concentrations up to $C_p/C^* \simeq 7$ and with different molecular weights M_p ranging from 17,500 to 88,000. An M_p-independent transition was indeed found when R_h becomes larger than ξ, as the theory suggested. However, the experiment also revealed several new features that cannot be explained by the simple scaling argument. It was found that when $R_h < \xi$, the particles "feel" the linear viscosity $\eta_0(1 + [\eta]C_p)$ of the solution rather than the solvent viscosity η_0. When $R_h \gg \xi$, the particles experience the macroscopic viscosity of the polymer solution, as suggested by the theory. In the transition region, the measured η_c/η_0 does not have the predicted scaling form $\varphi(R_h/\xi)$. Instead, a new switch function, $S_c(C_p) \equiv [\eta_c/\eta_0 - (1 + [\eta]C_p)]/[k_H([\eta]C_p)^2]$, is found to be of universal form independent of M_p.[35] Because the solution viscosity η_p, which is larger than η_c near $\tilde{C}_p$, is used in the Stokes−Einstein relation, a smaller η_c indicates a positive deviation from the SE relation. While a detailed theory is certainly needed in order to quantitatively describe the transitional behavior of the measured η_c/η_0, our sedimentation measurements clearly demonstrate that the $\eta_p(C_p)/\eta_c(C_p) > 1$ behavior shown in Figure 1 (i.e., positive deviations from the SE relation) is caused by the reduction of η_c when the particle size becomes comparable to or smaller than the correlation length ξ.

B. Probe Particles in an End-Adsorbing Polymer Solution. We now discuss the effect of polymer adsorption on the motion of the particles in a semidilute solution. The polymer adsorption can produce many types of polymer−colloid aggregates with different spatial configurations. In this section we discuss a simple case that the polymer chains can only end adsorb onto the colloidal surfaces. Our previous light and neutron scattering measurements on the fresh mixture samples (less than a month old) have shown,[28,29] that the PEP chains do not adsorb onto the colloidal surfaces, but the polar end group on the amine-PEP chains interacts attractively with the polar core of the particles. The amine-PEP chains were found to partition themselves between the bulk solution and the adsorbed state. Because of the surfactant corona around the colloidal cores, the polymer adsorption is mitigated and on average only one chain is adsorbed on a colloidal particle.[28,29] For the mixture samples used in this section, the number ratio of the particles to the polymer molecules is very small (varied from 0.25 to 0.015), and thus most amine-PEP chains are in the bulk solution. The colloid−amine-PEP mixture samples used in the measurements are all fresh ones prepared within 1−2 weeks. The fresh samples are used to avoid the effect of a slow secondary adsorption taking place over a time period of more than 3 months. This secondary adsorption process will be discussed in section IIIC.

Figure 3 shows the measured $v_c(C_p)\eta_p/[v_c(0)\eta_0]$ as a function of C_p for the amine-PEP with $M_p = 25{,}000$ (triangles) and $M_p = 40{,}000$ (diamonds). It is seen that the measured $v_c(C_p)\eta_p/[v_c(0)\eta_0]$ remains constant at unity in the whole range of C_p, indicating that the microscopic viscosity $\eta_c(C_p)$ overlaps with the solution viscosity $\eta_p(C_p)$, even when the particle size becomes smaller than ξ. Because the polymer adsorption takes place through an attractive interaction between the polar end group on the amine-PEP chain and the polar core of the particle, the effective radius of the resulting colloid−polymer micelles (on average, one chain per particle) is always larger than R_g. The correlation length ξ, on the other hand, is smaller than (when $C_p/C^* > 1$) or equal to (when $C_p/C^* \le 1$) R_g. As a result, the colloid−polymer micelles feel the viscosity of the polymer solution at all concentrations. This situation is different from that for the dilute polymer solution,

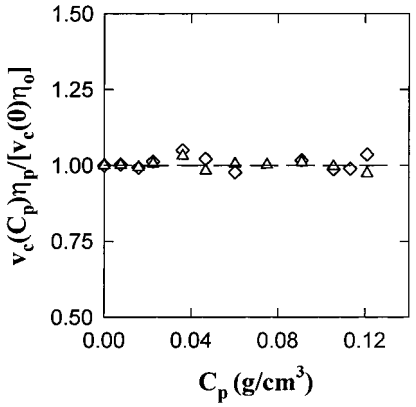

Figure 3. Measured $v_c(C_p)\eta_p/[v_c(0)\eta_0]$ as a function of C_p for the colloid−amine-PEP mixture samples with $M_p = 25{,}000$ (triangles) and $M_p = 40{,}000$ (diamonds). The dashed line indicates a constant baseline of unity.

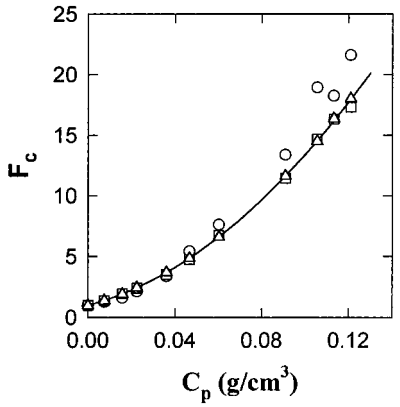

Figure 4. Measured F_c as a function of C_p for the colloid−amine-PEP mixture samples with $M_p = 40{,}000$. The squares are obtained from the sedimentation measurements. The circles are obtained from the scattering data with a second-order cumulant fit. The triangles are obtained from the same scattering data but with a triple exponential fit. The solid curve shows the viscosity of the polymer solution.

in which all the polymer chains are assumed to be adsorbed onto the colloidal surfaces and the solution viscosity becomes the same as the pure solvent. As mentioned in the above, in our colloid−amine-PEP mixture samples most polymer chains are in the bulk solution and only a small fraction of the polymer molecules are adsorbed onto the particles.

In the above measurements, η_c/η_0 is obtained from the velocity ratio $v_c(0)/v_c(C_p)$. It can also be obtained from the decay rate ratio $\Gamma(0)/\Gamma(C_p)$. The decay rate $\Gamma(C_p)$ of the measured correlation function $g(t)$ is related to the particle diffusion constant D_c in eq 1 via $\Gamma(C_p) = Q^2D_c(C_p)$. Figure 4 shows the measured $F_c \equiv \eta_c/\eta_0$ as a function of C_p for the amine-PEP with $M_p = 40{,}000$. The squares are obtained from the sedimentation data, which overlap well with the solution viscosity (the solid curve), as discussed above. The circles are obtained from the measurements of $g(t)$, and $\Gamma(C_p)$ is extracted from a second-order cumulant fit. It is seen that the scattering data coincide with the sedimentation data at low polymer concentrations and gradually become larger than the sedimentation data at higher C_p. In the cumulant analysis, the scattered light in the mixture sample is assumed to come all from the particles. In fact, as the polymer concentration is increased, contributions from the polymer scattering become increasingly important (the colloid concentration is fixed).

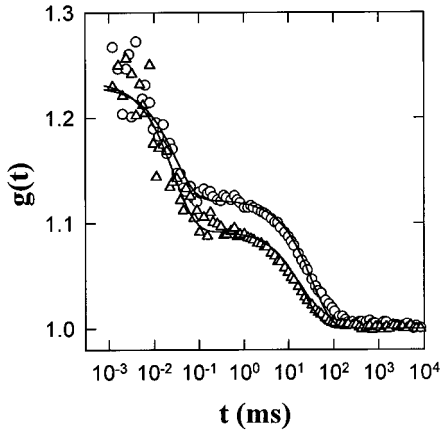

Figure 5. Measured $g(t)$ for the pure amine-PEP samples at $\theta = 90°$. The polymer molecular weight $M_p = 40{,}000$ and the concentrations are $C_p = 0.09$ g/cm^3 (triangles) and $C_p = 0.12$ g/cm^3 (circles). The solid curves are the least-squares fits by eqs 5 and 6.

Table 1. Fitting Results from the Pure Amine-PEP−Decane Samples

C_p (g/cm^3)	a_f	Γ_f (ms^{-1})	a_s	Γ_s (ms^{-1})
0.007	0.40	∼30	0.10	∼0.5
0.016	0.35	∼30	0.12	∼0.3
0.022	0.30	30	0.16	0.12
0.036	0.28	30	0.22	0.10
0.047	0.21	30	0.34	0.07
0.060	0.20	30	0.28	0.05
0.091	0.18	30	0.31	0.023
0.106	0.16	30	0.32	0.020
0.113	0.15	30	0.34	0.018
0.121	0.13	30	0.35	0.015

Figure 5 shows the measured $g(t)$ for the pure amine-PEP−decane samples with $M_p = 40{,}000$. The polymer concentrations are $C_p = 0.09$ g/cm^3 (triangles) and 0.12 g/cm^3 (circles). It is clearly seen that the measured $g(t)$ has two well-separated decay modes. The fast decay rate Γ_f is 3 orders of magnitude larger than the slow decay rate Γ_s. Because amine-PEP is a monodispersed polymer, the two decay modes in $g(t)$ are not caused by the size polydispersity of the samples.[40,41] Recent scattering experiments[29,28,34] have shown that there is no association found in the amine-PEP−decane solution. Therefore, it is unlikely that the two decay modes are originated from the presence of polymer clusters.[42] We believe that the two decay modes in $g(t)$ reflect the dynamics of the entangled polymer chains at different length scales.[43,44] To characterize the two decay modes, we use a double exponential function,

$$g_1(t) = a_f e^{-\Gamma_f t} + a_s e^{-\Gamma_s t} \tag{5}$$

to approximate the intensity correlation function $g(t)$. The measured $g(t)$ is related to $g_1(t)$ via the well-known equation[24]

$$g(t) = 1 + b|g_1(t)|^2 \tag{6}$$

where b (≤ 1) is an instrumental constant. The solid curves in Figure 5 show the least-squares fits by eqs 5 and 6. The fitting results are summarized in Table 1.

Because polymer scattering is very weak at low concentrations, the fitting results for the two most dilute samples have relatively large uncertainties. In Figure 6 we plot the apparent polymer diffusion constant $D_p \equiv \Gamma_s/Q^2$ as a function of C_p/C^*. For the amine-PEP with

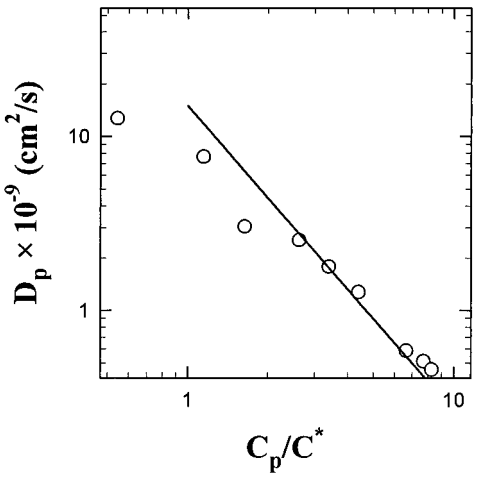

Figure 6. Fitted polymer diffusion constant D_p as a function of C_p/C^*. The solid line is the power law fit $D_p = 1.5 \times 10^{-8}$-$(C_p/C^*)^{-1.75}$ (cm^2/s).

$M_p = 40{,}000$, we have $R_g \simeq 10.5$ nm and $C^* \simeq 0.014$ g/cm^3. In the semidilute regime ($C_p/C^* > 1$), the data can be well described by a power law $D_p = 1.5 \times 10^{-8}$-$(C_p/C^*)^{\beta}$ (cm^2/s) (the solid line). The exponent $\beta = -1.75$ agrees with previous measurements.[45,46] In the above measurements the scattering wavenumber $Q = 0.02$ (nm^{-1}), and therefore $g(t)$ is measured in the long wavelength limit: $QR_g = 0.21 < 1$. It has been suggested that when $QR_g < 1$ and $C_p/C^* \geq 1$, Γ_s is related to the self-diffusion of the entangled polymer chains.[43,46,47] We notice, however, that the measured D_p in the dilute limit is at least 1 order of magnitude too small for the single chain diffusion (which can be calculated by using eq 1). This slow mode anomaly has also been observed in other polymer solutions[44−47] and is still not fully understood.

At small time scales, $g(t)$ contains information about the internal and pseudogel motions of the polymer chains.[43,44,47] However, because the polymer scattering is rather weak, the measured $g(t)$ at small t has larger scatters (see Figure 5). Consequently, the fitted Γ_f suffers relatively large experimental uncertainties. From the fitting we find that in the long wavelength limit, the fast decay mode is not very sensitive to C_p and can be adequately described by a constant Γ_f. It is seen from Table 1 that the fitted amplitude a_s increases with C_p, whereas a_f decreases with C_p. This is because ξ decreases with increasing C_p, and therefore large scale fluctuations become dominant in the high concentration samples. It should be pointed out that our main purpose here is to find an approximate functional form to analyze the scattering data from the mixture samples, rather than to study the polymer dynamics in the semidilute regime. Therefore, we use a triple exponential function

$$g_1(t) = a_c e^{-\Gamma_c t} + a_f e^{-\Gamma_f t} + a_s e^{-\Gamma_s t} \qquad (7)$$

to fit the measured $g(t)$ for the colloid−amine-PEP samples.

Figure 7 shows the measured $g(t)$ for the colloid−amine-PEP−decane mixture samples with $M_p = 40{,}000$. The polymer concentrations are $C_p = 0.007$ g/cm^3 (squares), 0.047 g/cm^3 (inverted triangles), and 0.113 g/cm^3 (hexagons). The solid curves are the least-squares fits by eqs 6 and 7. The fitting results are summarized in Table 2. In the fitting, the two polymer decay rates,

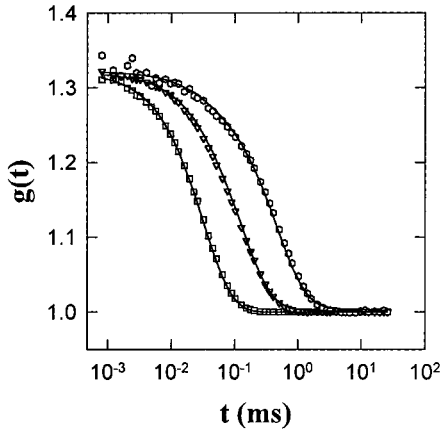

Figure 7. Measured $g(t)$ for the colloid−amine-PEP mixture samples at $\theta = 90°$. The polymer molecular weight $M_p = 40{,}000$ and the concentrations are $C_p = 0.007$ g/cm^3 (squares), 0.047 g/cm^3 (inverted triangles), and 0.113 g/cm^3 (hexagons). The solid curves are the least-squares fits by eqs 6 and 7.

Table 2. Fitting Results from the Colloid−Amine-PEP Mixture Samples

C_p (gm/cm^3)	a_c	Γ_c (ms^{-1})	a_f	Γ_f (ms^{-1})	a_s	Γ_s (ms^{-1})
0	0.54	19.64				
0.007	0.48	14.11	∼0.075	30	∼0.015	0.5
0.016	0.48	10.20	∼0.073	30	∼0.025	0.3
0.022	0.48	8.06	0.060	30	0.035	0.12
0.036	0.48	5.33	0.055	30	0.050	0.10
0.047	0.48	4.04	0.033	30	0.056	0.07
0.060	0.48	2.97	0.032	30	0.067	0.05
0.091	0.48	1.69	0.030	30	0.065	0.023
0.106	0.46	1.35	0.030	30	0.078	0.020
0.113	0.47	1.20	0.028	30	0.070	0.018
0.121	0.46	1.09	0.025	30	0.072	0.015

Γ_f and Γ_s, are kept the same as those in the pure polymer solutions and only the colloid decay rate Γ_c as well as the three amplitudes are allowed to vary. It is seen from Table 2 that the fitted colloid amplitude a_c for different C_p remains unchanged, because the colloid concentration of the mixture samples is kept the same. The polymer amplitudes, a_f and a_s, show the same trend as those in the pure polymer solutions. Because the polymer scattering at low C_p is much weaker than the colloid scattering, the fitting results for the two most dilute mixture samples are not sensitive to the polymer parameters. At higher polymer concentrations, however, the fitting becomes sensitive to the polymer parameters. The triangles in Figure 4 show the decay rate ratio $F_c = \Gamma_c(0)/\Gamma_c(C_p)$ obtained from the triple exponential fits. The fitted F_c now coincides well with the sedimentation data and with the viscosity of the polymer solution (the solid curve). Figure 4 thus suggests that the diffusion and sedimentation measurements provide the same information so long as the scattering measurement is carried out in the long wavelength limit: $QR_h < 1$ and $Q\xi < 1$. This condition requires that the motion of the probe particles be averaged over many particle configurations and over many correlation volumes of the polymer solution.[14] In the analysis of the measured correlation function $g(t)$, one needs to take polymer scattering into account for the high-C_p mixture samples.

In the literature,[14−19] the particle diffusion constant $D_c \equiv \Gamma_c/Q^2$ is often fitted by a stretched exponential function $D_c(C_p) = D_c(0)\exp[-(\gamma C_p)^{\nu}]$, where $D_c(0)$ is the particle diffusion constant in the pure solvent. Figure

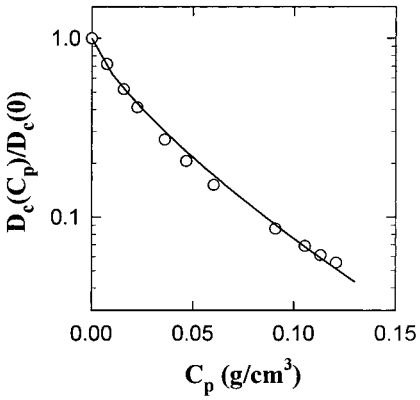

Figure 8. Normalized particle diffusion constant $D_c(C_p)/D_c(0)$ as a function of C_p for the colloid−amine-PEP mixture samples with $M_p = 40{,}000$. The solid curve is the fitted function $D_c(C_p)/D_c(0) = \exp[-(\gamma C_p)^\nu]$, with $D_c(0) = 5.08 \times 10^{-7}$ cm^2/s, $\gamma = 35.36$ cm^3/g, and $\nu = 3/4$.

8 shows the measured $D_c(C_p)/D_c(0)$ as a function of C_p for the colloid−amine-PEP mixture samples with $M_p = 40{,}000$. The solid curve is the fitted function $D_c(C_p)/D_c(0) = \exp[-(\gamma C_p)^\nu]$, with $D_c(0) = 5.08 \times 10^{-7}$ cm^2/s, $\gamma = 35.36$ cm^3/g, and $\nu = 3/4$. Because $D_c(0)/D_c(C_p) = \eta_p(C_p)/\eta_0$ in the colloid−amine-PEP samples (see Figure 4), the fitting in Figure 8 thus suggests that the stretched exponential function is another approximate expression for the viscosity of the polymer solution. In fact, Phillies and Peczak[48] have shown that the viscosity of many polymer solutions can be well described by a stretched exponential function. Our fit in Figure 8 agrees with their findings. The value of ν has been found to be in between 0.55 and 1 and our fitted value is 3/4. Many previous investigators have argued that $D_c(0)/D_c(C_p)$ should have a scaling form, and indeed, the fitted stretched exponential function can be converted to a simple exponential function $D_c(0)/D_c(C_p) = \exp[(\gamma C_p)^\nu] = \exp(R_g/\xi)$, once γ^{-1} is identified as C^*. In the adsorption case, however, the scaling variable is R_g/ξ instead of R_h/ξ. Similar behavior was also observed for the measured velocity ratio $v_c(0)/v_c(C_p)$ in the colloid−amine-PEP mixture samples with $M_p = 25{,}000$.[35] It was found that the stretched exponential function can only fit to the sedimentation data with adsorption but not to those without adsorption.

C. Probe Particles in a Cross-Linking Polymer Solution. In the measurements discussed in the previous section, the mixture samples used are all fresh ones prepared within 1−2 weeks. It is shown that the scattering and sedimentation data can be well described by considering the motion of individual colloid−polymer micelles with the polymer chains end-grafted on the colloidal surface. This situation, however, is changed completely for old colloid−amine-PEP samples, in which a gel is formed after a period of ∼3 months. Because the single-end amine group cannot form a cross-linked polymer network in the solution, the gelation must be induced by an additional adsorption of the PEP chains onto the colloidal surfaces. The particles, therefore, act like a cross-link agent for the gelation process. This conclusion is further supported by the following observations. First, there is no gelation found in the pure colloidal suspension and in the pure polymer solution. They are stable for at least 6 months, during which we have continued monitoring the samples. Therefore, the cross-link must result from the direct colloid−polymer interaction. Second, the gelation process is found to become somewhat faster and the resulting gel is stronger, when one increases either ϕ_c or C_p as well as M_p. The kinetics of the gelation process is very slow, because the surfactant corona around the colloidal cores mitigates the polymer adsorption. Increasing ϕ_c, C_p, or M_p will certainly enhance the cross-link probability. This speeds up the gelation process and produces a stronger gel.

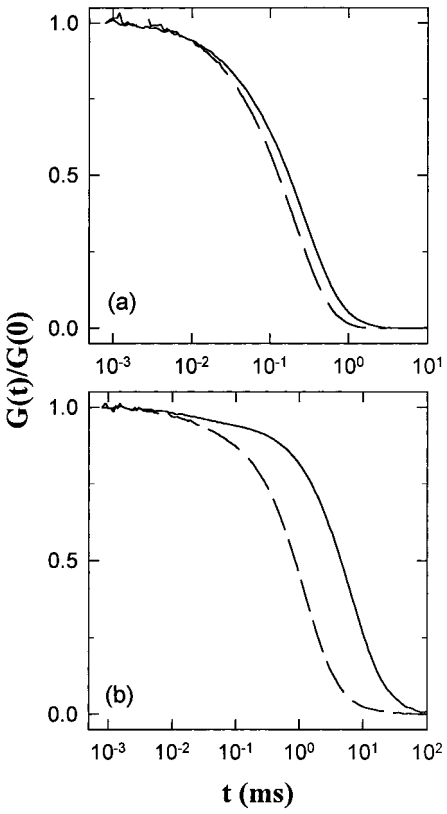

Figure 9. Normalized correlation function $G(t)/G(0)$ for the colloid−PEP mixture samples at $\theta = 90°$. The polymer molecular weight $M_p = 17{,}500$ and the concentrations are (a) $C_p = 0.06$ g/cm^3 and (b) $C_p = 0.12$ g/cm^3. The dashed curves are obtained from 1-year-old samples, and the solid curves are obtained 6 months later than the dashed curves.

One may expect that such a cross-link process between the colloidal core and the PEP chains may also take place in the colloid−PEP mixture samples. Indeed, we find that the old colloid−PEP samples behave differently from the fresh ones. Figure 9 compares the normalized correlation function $G(t)/G(0)$ [$G(t) \equiv g(t) - 1$] for the colloid−PEP samples measured at different times. The polymer concentrations are (a) $C_p = 0.06$ g/cm^3 and (b) $C_p = 0.12$ g/cm^3. The dashed curves are obtained from the 1-year-old samples and the solid curves are obtained 6 months later than the dashed curves. It is seen from Figure 9 that the decay rate Γ_c of $G(t)/G(0)$ is reduced considerably for the older samples. The amount of decrease in Γ_c is found to increase with C_p, M_p, and the sample age. By visually examining the mixture samples, we find that while they are somewhat viscoelastic, the solution can still flow when the sample cell is tilted. Because the polymer adsorption is much weaker in the absence of the amine end group, smaller polymer clusters are formed in the colloid−PEP solution. Increasing C_p, M_p, or simply waiting longer, will certainly enhance the growth of the polymer clusters. To examine the spatial distribution of the particles on the polymer cluster, we measure the scattered light

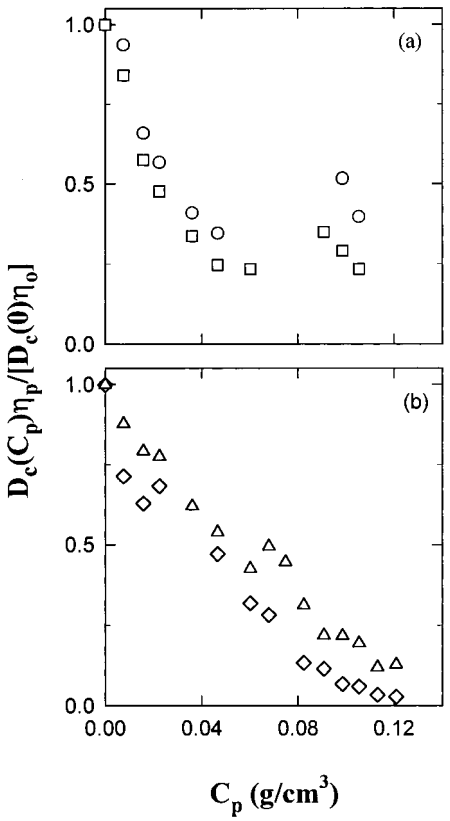

Figure 10. Measured $D_c(C_p)\eta_p/[D_c(0)\eta_0]$ as a function of C_p for the colloid−PEP mixture samples with (a) $M_p = 26{,}000$ and (b) $M_p = 17{,}500$. Both the circles in (a) and the triangles in (b) are obtained from 1-year-old samples. The squares in (a) are obtained 2 months later than the circles, and the diamonds in (b) are obtained 6 months later than the triangles.

intensity $I(Q)$ of the mixture samples as a function of Q. The measured $I(Q)$ is found to be the same as that for the pure colloidal suspension. This indicates that no large compact colloidal aggregates are formed in the solution and the particles are uniformly distributed on the polymer clusters.

Figure 10 shows the measured $D_c(C_p)\eta_p/[D_c(0)\eta_0]$ as a function of C_p for the colloid−PEP samples with (a) $M_p = 26{,}000$ and (b) $M_p = 17{,}500$. Both the circles in Figure 10a and the triangles in Figure 10b are obtained from 1-year-old samples. The squares in Figure 10a are obtained 2 months later than the circles, and the diamonds in Figure 10b are obtained 6 months later than the triangles. The diffusion constant $D_c(C_p)$ is obtained via $D_c(C_p) \equiv \Gamma_c/Q^2$, where Γ_c is extracted from a second-order cumulant fit to the measured $g(t)$. Figure 10 clearly shows that the large negative deviations from the SE relation are associated with the cross-link of the particles to the polymer cluster. In this case, the particles are not free to move in the solution, and $g(t)$ only measures the hindered local motion of the particles. As a result, Γ_c is no longer related to the local viscosity of the polymer solution, and eqs 1 and 2 are not valid anymore. It is seen from Figure 10 that D_c (or Γ_c) decreases with increasing C_p, M_p, and the sample age. All these effects can be explained by the fact that the polymer clusters have grown bigger and stronger, and they slow down the motion of the cross-linked particles.

IV. Conclusion

We have carried out a series of dynamic light scattering and sedimentation measurements to study the motion of small probe particles in neutral and adsorbing polymer solutions. By varying the microscopic interaction between the colloidal particle and the polymer molecule, we are able to observe three different behaviors towards the Stokes−Einstein (SE) equation in the same colloid−polymer system. Our sedimentation measurements in the nonadsorbing polymer solution clearly demonstrate that positive deviations from the SE relation are caused by the reduction of the local viscosity η_c felt by the particles when their size becomes comparable to or smaller than the correlation length ξ of the polymer solution. When $R_h < \xi$, the particles only "feel" the linear viscosity, $\eta_0(1 + [\eta]C_p)$, which is smaller than the solution viscosity η_p. Positive deviations from the SE relation have also been observed in other nonadsorbing colloid−polymer mixtures when $R_h \gg \xi$.[14] In these experiments, however, the dynamic light scattering measurements were carried out only in the regime $QR_g \simeq 1.5$ ($\theta = 90°$ is used to calculate Q). When $QR_g > 1$, dynamic light scattering can only measure the motion of the particles on a length scale smaller than R_g. The sedimentation experiment, on the other hand, probes the long-time behavior of the particle motion. The short-time motion of the particles could be influenced by local inhomogeneities of the medium, such as a polymer depletion layer around the particles.[14,20] Because the depletion layer thickness is approximately equal to the correlation length ξ,[49] which decreases with C_p, a return to the SE behavior is expected at higher polymer concentrations when $Q\xi < 1$. Indeed, this was observed in an experiment by Won et al.[14]

When the probe particles are suspended in an adsorbing polymer solution, the effect of polymer adsorption on the particle motion depends strongly on the spatial configuration of the resulting colloid−polymer aggregates. In the simple case that the polymer chains can only end-adsorb onto the colloidal surfaces, the particles are still free to move and no polymer clusters are formed in the solution. In this case, the end-grafted polymer chains make the effective radius of the colloid−polymer micelles always larger than ξ. This is true even when the radius of the bare particles is smaller than ξ. Our measurements in section IIIB reveal that the colloid−polymer micelles feel the solution viscosity at all polymer concentrations (i.e., adherence to the SE equation). As shown in section IIIA, when R_h becomes much larger than ξ, the particles experience the macroscopic viscosity of the polymer solution and the SE equation should apply at all polymer concentrations. Indeed, this was observed by Onyenemezu et al. in a nonadsorbing colloid−polymer mixture with $R_h \gg R_g$.[21] Their light scattering measurements were conducted under the long wavelength condition $QR_g \simeq 0.21$ ($\theta = 45°$ is used to calculate Q).

When the probe particles are attached to a polymer cluster by adsorption, their motion is hindered by the cross-linked polymer chains. In this case, the intensity correlation function $g(t)$ measures only the hindered local motion of the particles and its decay rate Γ_c is no longer related to the local viscosity η_c in the usual sense. Consequently, the SE equation becomes inapplicable. Our dynamic light scattering measurements for the old colloid−PEP mixture samples clearly show that negative deviations from the SE relation are associated with the cross-link of the particles to the polymer cluster. In previous experiments, the negative deviations from the SE relation have been ascribed to chain adsorption alone

causing an increase in R_h.[20] Our measurements in section IIIB reveal that there are no negative deviations found when the polymer chains can only end-adsorb onto the colloidal surfaces. The particles, in this case, experience the solution viscosity at all polymer concentrations. As shown in Figure 10b, the measured $D_c(C_p)\eta_p/[D_c(0)\eta_0]$ decreases with C_p down to 0.03 at the highest polymer concentration studied. This corresponds to a negative deviation from the SE equation by a factor of 33. Clearly, the particle's hydrodynamic radius cannot be increased by a factor 33 without bridging the particles with the polymer chains.

Acknowledgment. We have benefited from useful discussions with B. J. Ackerson and H. O. Spivey. We thank M. Y. Lin for his assistance in the neutron scattering measurement and acknowledge the National Institute of Standards and Technology for granting neutron beam times. This work was supported by the National Aeronautics and Space Administration under Grant No. NAG3-1852.

References and Notes

(1) Gittes, F.; Schnurr, B.; Olmsted, P. D.; MacKintosh, F. C.; Schmidt, C. F. *Phys. Rev. Lett.* **1997**, *79*, 3286 and references therein.
(2) Krall, A. H.; Huang, Z.; Weitz, D. A. *Physica A* **1997**, *235*, 19, and references therein.
(3) Durian, D. J. *Phys. Rev. Lett.* **1995**, *75*, 4780 and references therein.
(4) Mason, T. G.; Bibette, J.; Weitz, D. A. *Phys. Rev. Lett.* **1995**, *75*, 2051. Mason, T. G., et al., *Phys. Rev. E* **1997**, *56*, 3150 and references therein.
(5) Wirtz, D. *Phys. Rev. Lett.* **1995**, *75*, 2436.
(6) Amblard, F.; Maggs, A. C.; Yurke, B.; Pargellis, A. N.; Leibler, S. *Phys. Rev. Lett.* **1996**, *77*, 4470 and references therein.
(7) *Cytomechanics*; Bereiter-Hahn, J., Anderson, O. R., Reif, W.-E., Eds.; Springer: New York, 1987.
(8) *Cell Mechanics and Cellular Engineering*; Mow, V. C., Guilak, F., Tran-Son-Tay, R., Hochmuth, R. M., Eds.; Springer: New York, 1994.
(9) Amblard, F.; Yurke, B.; Pargellis, A. N.; Leibler, S. *Rev. Sci. Instrum.* **1996**, *67*, 818.
(10) Mason, T. G.; Ganesan, K.; van Zanten, J. H.; Wirtz, D.; Kuo, S. C. *Phys. Rev. Lett.* **1997**, *79*, 3282.
(11) Mason, T. G.; Gang, H.; Weitz, D. A. *J. Opt. Soc. Am. A* **1997**, *14*, 139.
(12) Barziv, R.; Meller, A.; Tlusty, T.; Moses, E.; Stavans, J.; Safran, S. A. *Phys. Rev. Lett.* **1997**, *78*, 154.
(13) de Gennes, P.-G. *Scaling Concepts in Polymer Physics*; Cornell University Press: Ithaca, NY, 1979.
(14) Won, J.; Onyenemezu, C.; Miller, W. G.; Lodge, T. P. *Macromolecules* **1994**, *27*, 7389 and references therein.
(15) Phillies, G. D. J. *J. Phys. Chem.* **1989**, *93*, 5029. Phillies, G. D. J.; Clomenil, D. *Macromolecules* **1993**, *26*, 167 and references therein.
(16) Langevin, D.; Rondelez, F. *Polymer* **1978**, *19*, 875.
(17) Brown, W.; Rymden, R. *Macromolecules* **1986**, *19*, 2942 and references therein.
(18) Russo, P. S.; Mustafa, M.; Cao, T.; Stephens, L. K. *J. Colloid Interface Sci.* **1988**, *122*, 120. Bu, Z.; Russo, P. S. *Macromolecules* **1994**, *27*, 1187 and references therein.
(19) Cooper, E. C.; Johnson, P.; Donald, A. M. *Polymer* **1991**, *32*, 2815.
(20) Gold, D.; Onyenemezu, C.; Miller, W. G. *Macromolecules* **1996**, *29*, 5700 and references therein.
(21) Onyenemezu, C.; Gold, D.; Roman, M.; Miller, W. G. *Macromolecules* **1993**, *26*, 3833 and references therein.
(22) Phillies, G. D. J.; Brown, W.; Zhou, P. *Macromolecules* **1992**, *25*, 4948 and references therein.
(23) Russel, W. B.; Saville, D. A.; Schowalter, W. R. *Colloidal Dispersions*; Cambridge University Press: Cambridge, U.K., 1989.
(24) Berne, B. J.; Pecora, R. *Dynamic Light Scattering*; Wiley: New York, 1976.
(25) Tong, P.; Witten, T. A.; Huang, J. S.; Fetters, L. J. *J. Phys. (France)* **1990**, *51*, 2813.
(26) Ye, X.; Narayanan, T.; Tong, P.; Huang, J. S. *Phys. Rev. Lett.* **1996**, *76*, 4640.
(27) Ye, X.; Narayanan, T.; Tong, P.; Huang, J. S.; Lin, M. Y.; Carvalho, B. L.; Fetters, L. J. *Phys. Rev. E* **1996**, *54*, 6500.
(28) Carvalho, B. L.; Tong, P.; Huang, J. S.; Witten, T. A.; Fetters, L. J. *Macromolecules* **1993**, *26*, 4632.
(29) Ye, X.; Tong, P.; Fetters, L. J. *Macromolecules* **1997**, *30*, 4103.
(30) Mays, J.; Hadjichristidis, N.; Fetters, L. *Macromolecules* **1984**, *17*, 2723.
(31) Mays, J.; Fetters, L. *Macromolecules* **1989**, *22*, 921.
(32) Davidson, N. S.; Fetters, L. J.; Funk, W. G.; Hadjichristidis, N.; Graessley, W. W. *Macromolecules* **1987**, *20*, 2614.
(33) Fetters, L. J.; Graessley, W. W.; Hadjichristidis, N.; Kiss, A. D.; Pearson, D. S.; Younghouse, L. B. *Macromolecules* **1988**, *21*, 1644.
(34) Davidson, N. S.; Fetters, L. J.; Funk, W. G.; Graessley, W. W.; Hadjichristidis, N. *Macromolecules* **1988**, *21*, 112.
(35) Tong, P.; Ye, X.; Ackerson, B. J.; Fetters, L. J. *Phys. Rev. Lett.* **1997**, *79*, 2363.
(36) Ye, X.; Tong, P.; Fetters, L. J. *Macromolecules*, in press.
(37) Vrij, A. *Pure Appl. Chem.* **1976**, *48*, 471.
(38) Daoud, M.; et al., *Macromolecules* **1975**, *8*, 804.
(39) Wiltzius, P.; Haller, H. R.; Cannell, D. S.; Schaefer, D. W. *Phys. Rev. Lett.* **1983**, *51*, 1183.
(40) Benmouna, M.; Benoit, H.; Duval, M.; Akcasu, Z. *Macromolecules* **1987**, *20*, 1107.
(41) Brown, J. C.; Pusey, P. N. *J. Chem. Phys.* **1975**, *62*, 1136.
(42) Zhou, P.; Brown, W. *Macromolecules* **1990**, *23*, 1131.
(43) de Gennes, P. G. *Macromolecules* **1976**, *9*, 587, 594. Brochard, F.; de Gennes, P. G. *Macromolecules* **1977**, *10*, 1157.
(44) Adam, M.; Delsanti, M. *Macromolecules* **1977**, *10*, 1229.
(45) Amis, E. J.; Han, C. C. *Polymer* **1982**, *23*, 1403.
(46) Doi, M.; Edwards, S. F. *The Theory of Polymer Dynamics*; Oxford: Oxford, U.K., 1986; p 171.
(47) Chu, B.; Nose, T. *Macromolecules* **1980**, *13*, 122.
(48) Phillies, G. D. J.; Peczak, P. *Macromolecules* **1988**, *21*, 214.
(49) Gast, A. P.; Leibler, L. *Macromolecules* **1986**, *19*, 686.

MA9801725